

From Chaos to Integrability in Double Scaled SYK

Micha Berkooz,^{*} Nadav Brukner,[†] and Yiyang Jia (贾抑扬)[‡]
*Department of Particle Physics and Astrophysics,
 Weizmann Institute of Science, Rehovot 7610001, Israel*

Ohad Mamroud[§]
SISSA, via Bonomea 265, 34136 Trieste, Italy[¶]
 (Dated: May 6, 2024)

We study thermodynamic phase transitions between integrable and chaotic dynamics. We do so by analyzing models that interpolate between the chaotic double scaled Sachdev-Ye-Kitaev (SYK) and the integrable p -spin systems, in a limit where they are described by chord diagrams. We develop a path integral formalism by coarse graining over the diagrams, which we use to argue that the system has two distinct phases: one is continuously connected to the chaotic system, and the other to the integrable. They are separated by a line of first order transition that ends at a critical point.

I. INTRODUCTION

Two important universality classes in quantum mechanics are those of *integrable* and *chaotic* systems, and the transition between these two behaviors is also of major interest. In this work we will focus on a universal dynamics which happens in such transitions in p -local quantum mechanical systems, such as the SYK system.

More precisely, we will be interested in a class of models that interpolate between chaotic and integrable p -local dynamics,

$$H = \nu H_{\text{Chaotic}} + \kappa H_{\text{Integrable}}, \quad \kappa^2 + \nu^2 = 1, \quad (1)$$

for $\kappa \in [0, 1]$, and ask whether one can find any thermodynamic phase transitions along the interpolation.

A measure of universality is obtained by focusing on systems with a *double scaling limit*. These are systems of N degrees of freedom, where we take $N, p \rightarrow \infty$ while keeping $\lambda = 2p^2/N$ fixed. The dynamics of such systems are governed by *chord diagrams* [1–5], to be defined below. As a concrete example, we choose two well known models as our two extremes:

On the chaotic end we have the Sachdev-Ye-Kitaev (SYK) model [6–9]—a disordered quantum mechanical model of N interacting Majorana fermions that exhibits various facets of quantum chaos, from level repulsion [10–12] to a maximal chaos exponent [6, 7, 13]. It has a rich history in nuclear physics [14, 15] and in condensed matter physics [8, 9] where it serves as a solvable example of a non-Fermi liquid, see [16] for a review. In the past decade it had gained attention in the high-energy physics community as an important controllable model of holography [6, 9, 12, 17–21].

On the other end we have the “commuting SYK” model [22, 23] – an integrable system of (even) N interacting fermions. It is better known as the integrable p -spin model [24–27] after a Jordan-Wigner transformation is used to write it as acting on a system of qubits. In the double scaling limit the model becomes the Random Energy model.

Below we show that the limit $\lambda \rightarrow 0$ is an emergent semi-classical limit, in which the system exhibits a first order phase transition at low temperatures T along $\kappa \propto \sqrt{T}$. It ends at some finite temperature in what is (presumably) a critical point. In a companion paper [28] we elaborate on our path integral approach and show that it can be used to analyze the phase diagram of generic systems in the aforementioned double scaling limit, amongst them the chaotic and integrable versions of the p -spin system. We also find cases where both systems are chaotic, but the interpolation exhibits a quantum phase transition at zero temperature.

II. THE MICROSCOPIC HAMILTONIAN

We consider a quantum mechanical system of (even) N Majorana fermions ψ_i , satisfying the anti-commutation relations $\{\psi_i, \psi_j\} = 2\delta_{ij}$. Our two Hamiltonians are

$$H_{\text{Chaotic}} = i^{p/2} \sum_{i_1 < \dots < i_p=1}^N J_{i_1 \dots i_p} \psi_{i_1} \dots \psi_{i_p}, \quad (2)$$

$$H_{\text{Integrable}} = i^{p/2} \sum_{i_1 < \dots < i_{p/2}=1}^{N/2} B_{i_1 \dots i_{p/2}} Q_{i_1} \dots Q_{i_{p/2}}, \quad (3)$$

with $Q_i = \psi_{2i-1} \psi_{2i}$ a fermion bilinear. The couplings are independent Gaussian random variables,

$$\langle J_I \rangle = 0, \quad \langle J_I J_K \rangle = \frac{1}{\lambda} \binom{N}{p}^{-1} \mathbb{J}^2 \delta_{IK}, \quad (4)$$

$$\langle B_L \rangle = 0, \quad \langle B_L B_M \rangle = \frac{1}{\lambda} \binom{N/2}{p/2}^{-1} \mathbb{J}^2 \delta_{LM}, \quad (5)$$

^{*} micha.berkooz@weizmann.ac.il

[†] nadav.brukner@weizmann.ac.il

[‡] yiyang.jia@weizmann.ac.il

[§] omamroud@sissa.it

[¶] Also at INFN, Sezione di Trieste, Via Valerio 2, 34127 Trieste, Italy

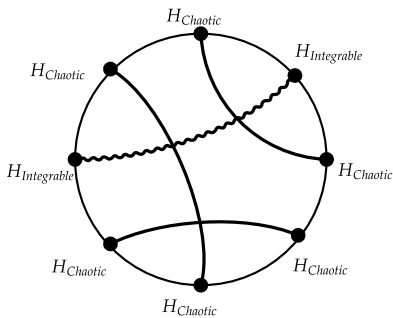


FIG. 1: A chord diagram with three n -chords and one z -chord. It contributes $\left(\frac{\mathbb{J}^2}{\lambda}\right)^4 \nu^6 \kappa^2 q^3$ to the moment m_8 .

where capital letters in the subscripts denote sets of indices, and the angular brackets denote the disorder averaging. In our normalization of the trace $\text{Tr}(\mathbb{1}) = 1$ [29] and $\langle \text{Tr}(H^2) \rangle = \mathbb{J}^2/\lambda$. We will be working with the units $c = \hbar = k_B = 1$.

A. Chord diagrams

In the double scaling limit the annealed [30] averaged partition function has a convenient diagrammatic expansion. First, the partition function with inverse temperature β , $Z = \langle \text{Tr}(e^{-\beta H}) \rangle$, is expanded into a series in the moments $m_k = \langle \text{Tr}(H^k) \rangle$. The disorder average of each moment can be computed by Wick's theorem and represented diagrammatically [1–5]—draw a circle with k nodes on its boundary, each representing an insertion of the Hamiltonian. Divide the nodes into $k/2$ pairs, and draw a chord connecting each pair. This is a *chord diagram*. The sum over all Wick contractions becomes a sum over all possible chord diagrams. In our case, since we have two types of random couplings, J and B , we have two types of chords, which we call n - and z -chords for the chaotic and integrable Hamiltonians respectively. An illustration appears in Figure 1.

Following [3], and as explained in Appendix B of the companion paper [28], in the double scaling limit the weight of the diagram is found as follows. Every n -chord contributes a factor of $(\nu^2 \mathbb{J}^2/\lambda)$ from the disorder averaging and the two Hamiltonian insertions associated with it. Every z -chord contributes $(\kappa^2 \mathbb{J}^2/\lambda)$. In addition, every intersection between n -chords contributes a factor of $q = e^{-\lambda}$, as do those between n -chords and z -chords. Intersections between z -chords are weighted by 1. If we denote the number of intersections between i - and j -chords in a diagram by X_{ij} , then the exact expression in the double scaling limit is

$$m_{2k} = \sum_{n+z=k} \sum_{C_{n,z}^k} \left(\frac{\mathbb{J}^2}{\lambda}\right)^k \nu^{2n} \kappa^{2z} q^{X_{nn}+X_{nz}}, \quad (6)$$

where $C_{n,z}^k$ represents the set of all chord diagrams with k chords, out of which n are n -chords and z are z -chords. Odd moments vanish due to the disorder average.

III. PATH INTEGRAL OVER CHORDS

In order to compute the partition function of the model we need to evaluate the sum over all chord diagrams with two types of chords, which is quite a formidable task. Luckily, the sum simplifies in the $\lambda \rightarrow 0$ limit—an emergent semi-classical limit controlled by diagrams with many chords. Our approach would be to coarse grain the system by dividing the boundary of the diagram into segments, and write the partition function as a sum over the number of chords of each kind that stretch between different segments. Each term in the sum is associated with many diagrams, and we will have to compute their collective weight. At the end, we will take a continuum limit where the number of segments, s , is very large. In this limit the i^{th} segment is identified with the Euclidean time τ_i , where $i/s = \tau_i/\beta$. This will result in a path integral expression for the partition function.

Let us begin. Arbitrarily divide the $2k$ Hamiltonian insertions in m_{2k} into s segments, each of length k_i . The moment computed using this division is denoted by $m_{\vec{k}}$, but since the division is arbitrary, $m_{\vec{k}} = m_{2k}$ for any \vec{k} . We average over the different divisions using $\frac{1}{s^{2k}} \sum_{\vec{k}} \binom{2k}{k_1, \dots, k_s} = 1$,

$$Z = \sum_{k=0}^{\infty} \frac{\beta^{2k}}{(2k)!} m_{2k} = \sum_{\vec{k}=0}^{\infty} \left[m_{\vec{k}} \prod_{i=1}^s \frac{(\beta/s)^{k_i}}{k_i!} \right]. \quad (7)$$

The insertions in each segment fall into different types: some belong to n - and z -chords that connect the i^{th} segment with the j^{th} segment, and hence we define

$$n_{ij}, z_{ij} - \text{No. of chords between } i^{\text{th}}, j^{\text{th}} \text{ segments.} \quad (8)$$

Eventually we will write the partition function as a sum over these variables. In total, each segment has $n_i = \sum_j n_{ij}$ n -chords and $z_i = \sum_j z_{ij}$ z -chords connecting it to other segments. There are also chords connecting the segment to itself, \hat{n}_i and \hat{z}_i chords of each kind, which come with twice as many insertions.

The coarse grained classes of chord diagrams are characterized by different possible divisions of each k_i into these kinds of chords, constrained by $k_i = n_i + z_i + 2\hat{n}_i + 2\hat{z}_i$. To compute $m_{\vec{k}}$ we therefore need to sum over these divisions, and we do so with the following weights, illustrated in Figure 2. We will evaluate the leading non-trivial order for each of these factors in the limit $\lambda \rightarrow 0$.

The first factor counts all the possible ways to **generate** the chords that leave the segment, i.e., their possible placement within the segment and their possible intersections with the chords that connect the segment to itself.

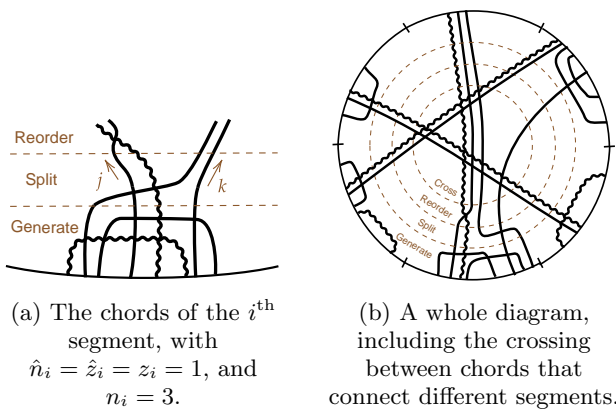


FIG. 2: An illustration of the terms that are considered in each part of the coarse graining procedure.

There are $\binom{k_i}{n_i, z_i, 2\hat{n}_i, 2\hat{z}_i}$ ways of choosing which nodes belong to each group of chords in each segment. Then, there are $(2\hat{n}_i - 1)!! = \frac{(2\hat{n}_i)!}{2^{\hat{n}_i} \hat{n}_i!}$ ways of connecting the $2\hat{n}_i$ nodes, as the first could be connected to any of the other $2\hat{n}_i - 1$, the third to any of the remaining $2\hat{n}_i - 3$ and so on. An additional factor of $(2\hat{z}_i - 1)!!$ comes from the z -nodes. We also remind the readers that the factors associated with each insertion give $\left(\frac{\nu\mathbb{J}}{\sqrt{\lambda}}\right)^{n_i+2\hat{n}_i} \left(\frac{\kappa\mathbb{J}}{\sqrt{\lambda}}\right)^{z_i+2\hat{z}_i}$ for each segment.

The second factor comes from the different ways we can **split** in each segment the n_i outgoing chords into the subsets $\{n_{ij}\}$, i.e., to decide which n -chords connect to every other segment, and similarly for the z -chords. There are $\binom{n_i}{n_{i1}, \dots, n_{is}} \binom{z_i}{z_{i1}, \dots, z_{is}}$ ways of doing so.

The third counts the ways we can **reorder** the n_{ij} , z_{ij} chords connecting every two segments—the ways in which they could intersect themselves. There are $n_{ij}! z_{ij}!$ such ways, and this factor needs to be counted once for every pair of segments i and j .

Finally, the last factor weights the bulk **crossings** of the chords that connect different segments, see Figure 2b,

$$\prod_{i < k < j < \ell} q^{n_{ij}n_{k\ell} + n_{ij}z_{k\ell} + n_{k\ell}z_{ij}}. \quad (9)$$

$$S = \frac{1}{4} \int_0^\beta d\tau_1 \int_0^\beta d\tau_2 \int_{\tau_1}^{\tau_2} d\tau_3 \int_{\tau_2}^{\tau_1} d\tau_4 \left\{ n(\tau_1, \tau_2)n(\tau_3, \tau_4) + 2n(\tau_1, \tau_2)z(\tau_3, \tau_4) \right\} \\ + \frac{1}{2} \int_0^\beta d\tau_1 \int_0^\beta d\tau_2 \left\{ n(\tau_1, \tau_2) \left[\log \left(\frac{n(\tau_1, \tau_2)}{\nu^2 \mathbb{J}^2} \right) - 1 \right] + z(\tau_1, \tau_2) \left[\log \left(\frac{z(\tau_1, \tau_2)}{\kappa^2 \mathbb{J}^2} \right) - 1 \right] \right\}. \quad (13)$$

The τ 's live on a circle of length β , and flipping the limits of the integration is understood as integrating over the other side of the circle. The pre-factors correct the overcounting when switching τ_1 and τ_2 , and when switching

Putting all of these factors together and performing the sum over the chords that are restricted to a single segment, \hat{n}_i and \hat{z}_i , we find

$$Z = e^{\frac{(\beta\mathbb{J})^2}{2\lambda s}} \sum_{\{n_{ij}\}, \{z_{ij}\}} \left\{ q^{\sum_{i < k < j < \ell} [n_{ij}n_{k\ell} + n_{ij}z_{k\ell} + z_{ij}n_{k\ell}]} \right. \\ \left. \times \prod_{j > i=1}^s \frac{1}{n_{ij}! z_{ij}!} \left(\frac{\nu^2 \beta^2 \mathbb{J}^2}{\lambda s^2} \right)^{n_{ij}} \left(\frac{\kappa^2 \beta^2 \mathbb{J}^2}{\lambda s^2} \right)^{z_{ij}} \right\}. \quad (10)$$

Note that we have not taken the strict $\lambda \rightarrow 0$ limit in every factor. The reason for that comes from the continuum limit we will soon take, where the segments are very small. The bulk crossings term (9) encodes correlations between regions with large (Euclidean) time separation, and we keep their λ dependence. On the other hand, the other factors are related to chords that are very close to each other, and therefore captures in some sense the short time behavior of the chords. The number of intersections here can be made small in the subsequent continuum limit, and we take $\lambda \rightarrow 0$. Our approach balances between these behaviors.

The partition function simplifies considerably by taking two limits. First, assuming a large number of chords, $n_{ij}, z_{ij} \gg 1$. This is self consistent at the saddle point when $\lambda \rightarrow 0$. The limit allows us to approximate the factorials by Stirling's formula, $n! \xrightarrow{n \rightarrow \infty} e^{n(\log n - 1)}$. Second, we take the continuum limit $s \rightarrow \infty$, as alluded to before. By introducing the continuum chord density fields, which are now functions of the Euclidean times,

$$n(\tau_i, \tau_j) = \frac{\lambda s^2}{\beta^2} n_{ij}, \quad z(\tau_i, \tau_j) = \frac{\lambda s^2}{\beta^2} z_{ij}, \quad (11)$$

we end up with a path integral expression for the partition function,

$$Z = \int \mathcal{D}n \mathcal{D}z e^{-\frac{1}{\lambda} S[n, z]}, \quad (12)$$

with a flat measure over all non-negative, symmetric, and periodic functions of two variables, and with the action

the pairs $\tau_{1,2}$ and $\tau_{3,4}$.

In our $\lambda \rightarrow 0$ limit the integral is controlled by its

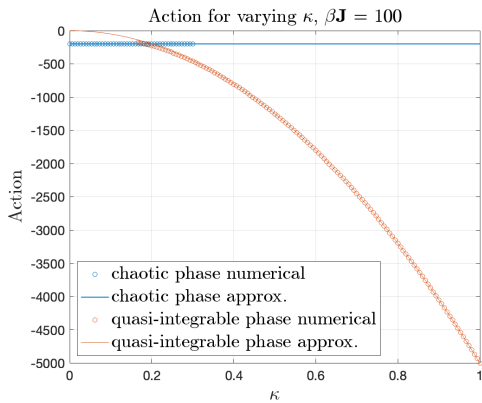


FIG. 3: Comparison of the numerics vs leading order approximation for the action of the two phases.

saddle point. We introduce the fields

$$g_n(\tau_1, \tau_2) = - \int_{\tau_1}^{\tau_2} d\tau_3 \int_{\tau_2}^{\tau_1} d\tau_4 n(\tau_3, \tau_4), \quad (14)$$

$$g_z(\tau_1, \tau_2) = - \int_{\tau_1}^{\tau_2} d\tau_3 \int_{\tau_2}^{\tau_1} d\tau_4 z(\tau_3, \tau_4), \quad (15)$$

that have period β in both variables and satisfy

$$g_n(\tau, \tau) = g_z(\tau, \tau) = 0, \quad (16)$$

and the saddle point equations read

$$\partial_{\tau_1} \partial_{\tau_2} g_n(\tau_1, \tau_2) = -2\mathbb{J}^2 \nu^2 e^{g_n(\tau_1, \tau_2) + g_z(\tau_1, \tau_2)}, \quad (17)$$

$$\partial_{\tau_1} \partial_{\tau_2} g_z(\tau_1, \tau_2) = -2\mathbb{J}^2 \kappa^2 e^{g_n(\tau_1, \tau_2)}. \quad (18)$$

When $\kappa = 0$ the equations of motion and the resulting partition function reproduce those of the $G\Sigma$ approach in the large interaction length [7] and double scaling [12, 31] limits, but it is important to note that our off-shell action is different than theirs.

IV. FROM CHAOS TO INTEGRABILITY

The saddle point equations can be solved numerically, and are found to have two types of solutions: one, the chaotic phase, is continuously connected to the saddle of the chaotic system at $\kappa = 0$. The other, which we call the quasi-integrable phase, is connected to the saddle point of the integrable system at $\kappa = 1$. We stress that the names only reflect the relation to the pure integrable and chaotic solutions, and nothing more. At low enough temperatures both solutions exist for some range of κ and change their dominance as we increase it, which results in a first order phase transition, see Figure 3.

At low temperatures, $\beta\mathbb{J} \gg 1$, the existence of the phase transition can be explained by the perturbative solutions around the two extremes. To leading order in

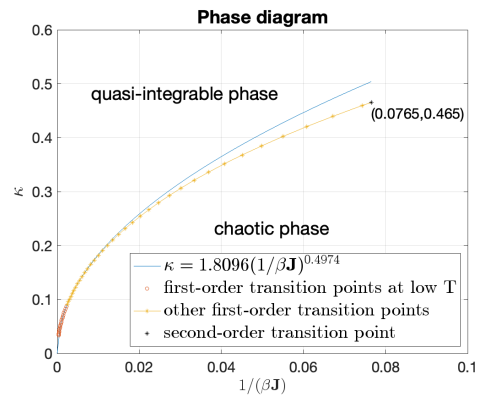


FIG. 4: Phase diagram in the $\kappa - 1/\beta\mathbb{J}$ plane. The red and yellow dots are first-order phase transition points. The former are in the low temperature region, and only they are used to obtain the power-law fit (blue). The first-order transition line terminates at the black dot.

both κ and $\beta\mathbb{J}$, the solution around $\kappa = 0$ is

$$g_n^{\kappa=0}(\tau_1, \tau_2) = 2 \log \left[\frac{\pi}{\beta\mathbb{J} \cos \left[\pi \left(\frac{1}{2} - \frac{|\tau_1 - \tau_2|}{\beta} \right) \right]} \right], \quad (19)$$

$$g_z^{\kappa=0}(\tau_1, \tau_2) = 0. \quad (20)$$

On the other hand, around $\kappa = 1$ the solution is

$$g_n^{\kappa=1}(\tau_1, \tau_2) = 0, \quad (21)$$

$$g_z^{\kappa=1}(\tau_1, \tau_2) = -(\mathbb{J}\kappa)^2 \tau(\tau - \beta). \quad (22)$$

The two solutions have the actions

$$S_{\kappa=0} = -2\beta\mathbb{J}, \quad S_{\kappa=1} = -\frac{1}{2}(\beta\mathbb{J}\kappa)^2. \quad (23)$$

We give more details about the perturbative solutions in the companion paper [28]. Importantly, we show that the subleading corrections around $\kappa = 1$ are suppressed at low temperatures. This enhances the range of validity for the approximation, and allows us to connect it to the one around $\kappa = 0$.

The phase transition happens when the two actions are equal. The above approximations set this point at

$$\kappa_* = \frac{2}{\sqrt{\beta\mathbb{J}}}. \quad (24)$$

This low-temperature estimate fits the numerical results summarized in Figure 4 quite well—the power law is precisely matched, and the numerical coefficient agrees to within 10%. At fixed κ , the low temperature phase is the integrable phase. At higher temperatures our analytic approximations are no longer accurate, and the numerics show that the phase transition line ends at finite temperature and κ , presumably in a second order fixed point.

V. DISCUSSION

The double scaling limit is a robust universal limit for many p -local systems. The results of this paper show that in this class of models, described by chord diagrams, there is a semi-classical description whose saddle point is controlled by coupled Liouville equations. This presents a generalization of the collective field ($G\Sigma$) approach to the case of multiple Hamiltonians in the double scaling limit.

It is interesting that coupled Liouville equations are the generic description of such systems. Systems of coupled Liouvilles often have additional symmetries, and it would be interesting to see if there are additional structures like a generalized Schwarzian. The strong exponential dependence of the field almost guarantees that the system will be governed by first order phase transitions since it is difficult (but not impossible) to balance the exponentials.

Indeed, we find that there is a first order phase transition that separates the chaotic phase from a quasi-integrable phase. Perhaps the abrupt transition between the two phases should not surprise us, as previous studies have found a discontinuous behavior of the chaos exponent when deforming integrable systems in quantum mechanical and field theoretical models [32, 33], which is somewhat reminiscent of the KAM theorem in classical systems.

One might wonder what happens to these systems away from the double scaling limit, at finite p . Other works have studied integrable deformations of the SYK model [34–38], in part as controllable models for transitions between thermalizing and many body localized systems. In the finite p version of our Hamiltonian (1) there is also sometimes a glassy phase, and so it could

provide an arena to study the interplay between chaos, integrability and the glass transition.

Finally, we note that SYK-like systems could also be studied experimentally [39] or by quantum simulations [40]. It is therefore important to verify that such realizations are in the correct phase. It is exciting to hope that the phase transition itself could be studied in the lab.

ACKNOWLEDGMENTS

We would like to thank Ahmed Almheiri, Dionysios Anninos, Andreas Blommaert, Ronny Frumkin, Damian Galante, Antonio García-García, Vladimir Narovlansky, and Josef Seitz for useful discussions. YJ also thanks Chi-Ming Chang and Zhenbin Yang for their invitation to visit Yau Mathematical Sciences Center (YMSC) and Institute for Advance Studies at Tsinghua University (IASTU), where part of this work is done. This work was supported in part by an Israel Science Foundation (ISF) center for excellence grant (grant number 2289/18), by ISF grant no. 2159/22, by the Minerva foundation with funding from the Federal German Ministry for Education and Research, by the German Research Foundation through a German-Israeli Project Cooperation (DIP) grant “Holography and the Swampland”. YJ is also supported by the Koshland postdoctoral fellowship and by a research grant from Martin Eisenstein. OM is supported by the ERC-COG grant NP-QFT No. 864583 “Non-perturbative dynamics of quantum fields: from new deconfined phases of matter to quantum black holes”, by the MUR-FARE2020 grant No. R20E8NR3HX “The Emergence of Quantum Gravity from Strong Coupling Dynamics”. OM is also partially supported by the INFN “Iniziativa Specifica GAST”.

-
- [1] L. Erdős and D. Schröder, *Math. Phys. Anal. Geom.* **17**, 441 (2014), [arXiv:1407.1552 \[math-ph\]](#).
 - [2] M. Berkooz, P. Narayan, and J. Simon, *JHEP* **08**, 192 (2018), [arXiv:1806.04380 \[hep-th\]](#).
 - [3] M. Berkooz, M. Isachenkov, V. Narovlansky, and G. Torrents, *JHEP* **03**, 079 (2019), [arXiv:1811.02584 \[hep-th\]](#).
 - [4] A. M. García-García, Y. Jia, and J. J. Verbaarschot, *JHEP* **2018**, 146 (2018).
 - [5] Y. Jia and J. J. M. Verbaarschot, *JHEP* **11**, 031 (2018), [arXiv:1806.03271 \[hep-th\]](#).
 - [6] A. Kitaev, “A simple model of quantum holography,” KITP strings seminar and Entanglement 2015 program, 12 February, 7 April and 27 May 2015, <http://online.kitp.ucsb.edu/online/entangled15/>.
 - [7] J. Maldacena and D. Stanford, *Phys. Rev. D* **94**, 106002 (2016), [arXiv:1604.07818 \[hep-th\]](#).
 - [8] S. Sachdev and J. Ye, *Phys. Rev. Lett.* **70**, 3339 (1993).
 - [9] A. Sachdev, *Phys. Rev. Lett.* **105**, 151602 (2010).
 - [10] Y.-Z. You, A. W. W. Ludwig, and C. Xu, *Phys. Rev. B* **95**, 115150 (2017), [arXiv:1602.06964 \[cond-mat.str-el\]](#).
 - [11] A. M. García-García and J. J. M. Verbaarschot, *Phys. Rev. D* **94**, 126010 (2016).
 - [12] J. S. Cotler, G. Gur-Ari, M. Hanada, J. Polchinski, P. Saad, S. H. Shenker, D. Stanford, A. Streicher, and M. Tezuka, *JHEP* **05**, 118 (2017), [Erratum: *JHEP* **09**, 002 (2018)], [arXiv:1611.04650 \[hep-th\]](#).
 - [13] J. Maldacena, S. H. Shenker, and D. Stanford, *JHEP* **08**, 106 (2016), [arXiv:1503.01409 \[hep-th\]](#).
 - [14] J. French and S. Wong, *Physics Letters B* **33**, 449 (1970).
 - [15] O. Bohigas and J. Flores, *Physics Letters B* **34**, 261 (1971).
 - [16] D. Chowdhury, A. Georges, O. Parcollet, and S. Sachdev, *Rev. Mod. Phys.* **94**, 035004 (2022), [arXiv:2109.05037 \[cond-mat.str-el\]](#).
 - [17] J. Maldacena, D. Stanford, and Z. Yang, *PTEP* **2016**, 12C104 (2016), [arXiv:1606.01857 \[hep-th\]](#).
 - [18] P. Saad, S. H. Shenker, and D. Stanford, (2018), [arXiv:1806.06840 \[hep-th\]](#).
 - [19] J. Maldacena and X.-L. Qi, (2018), [arXiv:1804.00491 \[hep-th\]](#).
 - [20] K. Jensen, *Phys. Rev. Lett.* **117**, 111601 (2016), [arXiv:1605.06098 \[hep-th\]](#).

- [21] J. Polchinski and V. Rosenhaus, *JHEP* **04**, 001 (2016), [arXiv:1601.06768 \[hep-th\]](#).
- [22] P. Gao, *JHEP* **01**, 149 (2024), [arXiv:2306.14988 \[hep-th\]](#).
- [23] A. Almheiri, A. Goel, and X.-Y. Hu, (2024), [arXiv:2403.18333 \[hep-th\]](#).
- [24] B. Derrida, *Phys. Rev. Lett.* **45**, 79 (1980).
- [25] B. Derrida, *Phys. Rev. B* **24**, 2613 (1981).
- [26] D. Gross and M. Mezard, *Nuclear Physics B* **240**, 431 (1984).
- [27] E. Gardner, *Nuclear Physics B* **257**, 747 (1985).
- [28] M. Berkooz, N. Brukner, Y. Jia, and O. Mamroud, (2024), [arXiv:2403.05980 \[hep-th\]](#).
- [29] The natural normalization for the trace, $\text{Tr}(\mathbb{1}) = 2^{N/2}$, simply multiplies the partition function (and the moments) by that overall factor.
- [30] For SYK, the system self averages to leading order in N [41]. For the integrable system there is a glassy phase transition [27], but in the double scaling limit it happens at temperature of order $\mathbb{J}/(\lambda N) \rightarrow 0$, and so the annealed averaging is justified. We assume that there is no glassy phase at any point along the interpolation.
- [31] D. Stanford, “Talk at [kitp](#),” (2018).
- [32] M. Berkooz, A. Sharon, N. Silberstein, and E. Y. Urbach, *Phys. Rev. D* **106**, 045007 (2022), [arXiv:2111.06108 \[hep-th\]](#).
- [33] M. Berkooz, A. Sharon, N. Silberstein, and E. Y. Urbach, *Phys. Rev. Lett.* **129**, 071601 (2022), [arXiv:2207.11980 \[hep-th\]](#).
- [34] S. Banerjee and E. Altman, *Physical Review B* **95**, 134302 (2017).
- [35] C.-M. Jian, Z. Bi, and C. Xu, *Physical Review B* **96**, 115122 (2017).
- [36] S.-K. Jian and H. Yao, *Phys. Rev. Lett.* **119**, 206602 (2017), [arXiv:1703.02051 \[cond-mat.str-el\]](#).
- [37] A. M. García-García, B. Loureiro, A. Romero-Bermúdez, and M. Tezuka, *Phys. Rev. Lett.* **120**, 241603 (2018), [arXiv:1707.02197 \[hep-th\]](#).
- [38] C. Peng, *JHEP* **05**, 129 (2017), [arXiv:1704.04223 \[hep-th\]](#).
- [39] D. I. Pikulin and M. Franz, *Phys. Rev. X* **7**, 031006 (2017), [arXiv:1702.04426 \[cond-mat.dis-nn\]](#).
- [40] D. Jafferis, A. Zlokapa, J. D. Lykken, D. K. Kolchmeyer, S. I. Davis, N. Lauk, H. Neven, and M. Spiropulu, *Nature* **612**, 51 (2022).
- [41] S. Sachdev, *Phys. Rev. X* **5**, 041025 (2015), [arXiv:1506.05111 \[hep-th\]](#).